Scanning Microscopy

Volume 10 | Number 2 Article 7

3-3-1996

Regenerating Synovial Lining of the Normal Rabbit Knee: A Scanning Electron Microscopy Study

Haim Stein
Technion-Israel Institute of Technology

Daniel Levanon
Technion-Israel Institute of Technology

Follow this and additional works at: https://digitalcommons.usu.edu/microscopy

 Part of the Biology Commons

Recommended Citation

Stein, Haim and Levanon, Daniel (1996) "Regenerating Synovial Lining of the Normal Rabbit Knee: A Scanning Electron Microscopy Study," *Scanning Microscopy*: Vol. 10 : No. 2 , Article 7.
Available at: https://digitalcommons.usu.edu/microscopy/vol10/iss2/7

This Article is brought to you for free and open access by the Western Dairy Center at DigitalCommons@USU. It has been accepted for inclusion in Scanning Microscopy by an authorized administrator of DigitalCommons@USU. For more information, please contact digitalcommons@usu.edu.

Scanning Microscopy, Vol. 10, No. 2, 1996 (Pages 371-384) 0891-7035/96$5.00+.25
Scanning Microscopy International, Chicago (AMF O'Hare), IL 60666 USA

REGENERATING SYNOVIAL LINING OF THE NORMAL RABBIT KNEE: A SCANNING ELECTRON MICROSCOPY STUDY

Haim Stein[1,2] and Daniel Levanon[1,*]

[1]The Bruce Rappaport Faculty of Medicine, Technion-Israel Institute of Technology, Haifa, 31096 Israel
[2]Department of Orthopedic Surgery, Rambam Medical Center, Haifa, 31096 Israel

(Received for publication March 9, 1995 and in revised form March 3, 1996)

Abstract

Regeneration of the synovial lining in the synovectomized rabbit knee was studied using the scanning electron microscope. The resected synovia regenerated considerably 3 weeks after synovectomy. However, 44 weeks following excision, their surface morphology was still very different from that of the normal tissue of intact animals. The regenerated synovia were characterized by three main features: the large number of various patterns, the many fields harboring fibrillation and the almost total lack of a bubble layer (the latter was formerly shown to be predominant on normal, intact synovia). The surface morphology of the non-operated (contralateral) knee differed greatly from that of normal synovia. The surface of sham-operated synovia was totally covered by the bubble layer. The appearance of vast fields harboring fibrillations indicated deficient ultrastructural regeneration. The altered surface morphology of the contralateral synovia was a novel finding. We wonder whether it would be appropriate to propose that the systemic reaction induced by synovectomy of the experimental knee initiated the synovial appearances recorded on the contralateral knee. The data reported here rule out the possibility of using the contralateral leg as an intact control.

Key Words: Synovial linings, rabbit, knee, scanning electron microscopy, synovectomy, regeneration, biomechanical incongruity in knee, fibrillation, contralateral leg, tannic acid.

*Address for correspondence:
Daniel Levanon
Unit of Electron Microscopy,
Faculty of Medicine, Technion,
P.O.B. 9649,
31096 Haifa, Israel
Telephone number: 972 (04) 829-5367
FAX number: 972 (04) 8514-285

Introduction

Synovectomy is applied in the treatment of rheumatoid arthritis and other arthritides of the knee. Despite having been in routine clinical use during different periods, the therapeutic value and prospects of knee synovectomy are currently under renewed consideration (McEwen, 1988; Gardner, 1991). Only a few inconclusive reports about the course of synovial morphological regeneration have appeared (Mitchell and Blackwell, 1968; Geens, 1969; Laurin *et al.*, 1974; Bently *et al.*, 1975; Stein, 1976; Myllala *et al.*, 1983; Frizziero *et al.*, 1992). However, this knowledge is important for the assessment of restoration of synovial structure and function (Lohmander, 1991). A close similarity in the ultrastructure of human and rabbit healthy synovial linings has been documented (Ghadially, 1983). This suggests that studying the surface morphology of the regenerating synovial lining in the rabbit knee might add information of both basic and clinical value regarding human synovial restoration.

In a previous article (Levanon and Stein, 1992), we described the surface morphology of the synovial lining of the intact healthy rabbit knee using specimens reinforced by tannic acid. The latter agent was found to enhance the preservation of synovial surface components that could not be demonstrated in the scanning electron microscope (SEM) by other procedures. In the present study, using the same protocol, we describe in detail the surface morphology of regenerating synovial linings in the normal, healthy rabbit.

Materials and Methods

Fifteen healthy albino rabbits (with a male/female ratio of 1:1) of local breed, averaging 1.8 kg, underwent subtotal synovectomy of their right knee, as described by Mitchell and Blackwell (1968). The rabbits were allowed to recover from anesthesia and then returned to lodge cages, with space to move around freely and food and water given *ad libitum*. Within 2-3 days after the operation, the rabbits moved easily, although even after

Table 1. Gross patterns of synovial-lining surface morphology in rabbits.

Pattern/ Figure No.	Healing Time	Leg	Anatomical Sector	Description
2A	3 weeks	Con	Medial	Accordion; ridges narrow and tightly packed; straight and/or curled ridges
2B	3 weeks	Syn	Medial	Flat areas without distinct organization; occasional synoviophytes
3	16 weeks	Syn	Medial	Flat areas with adjacent gross and/or fine, loosely or tightly packed accordion ridges with changing orientations
4	17 weeks	Syn	Lateral	Accordion ridges over whole synovial surface, with alternating orientations; in some places, tears occur on the surface and disclose sieve bundles from underneath
5	17 weeks	Con	Lateral	Fatty areolar; in some places, lack of interfibrillar material on vast or small fields
6	29 weeks	Syn	Lateral	Flat or semi-flat surfaces without distinct organization, "rusty" in places, with gross adipocytes
7	20 weeks	Con	Lateral	Lobe-like

Con = contralateral control knee; Syn = synovectomized (right) knee

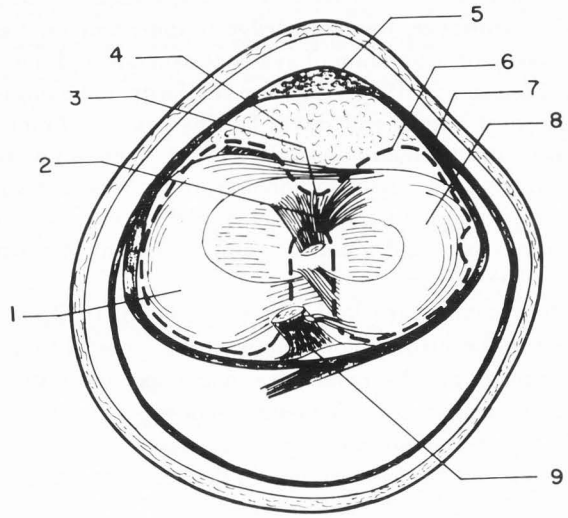

Figure 1. The diagram represents: 1: medial meniscus, 2: anterior cruciate ligament, 3: infrapatellar fold of synovial membrane, 4: infrapatellar fat pad, 5: patellar ligament, 6: synovial lining, 7: joint capsule, 8: lateral meniscus and 9: posterior cruciate ligament.

another 7-10 days, they were still seen frequently bearing some of their body weight on the left, intact leg. Animals were killed by an overdose of pentobarbital at defined time intervals of 3-44 weeks. Two rabbits were sham operated and allowed to recover for 8 weeks, after which they were killed and their synovia were obtained and analyzed. Medial and lateral specimens were resected and prepared for the SEM, as previously described (Levanon and Stein, 1992). The synovial specimens could be reliably separated from adjacent tissue, stretched on a porous plastic undersurface and prepared for the SEM without disintegration or any obvious harm.

Specimens were fixed in 2% glutaraldehyde in phosphate-buffered saline (PBS), pH 7, for 2-5 hours at room temperature and then overnight at 4°C. They were rinsed in PBS, treated with 2% tannic acid and 2% guanidine-HCl for 1 hour according to the GTGO method of Gamliel *et al.* (1983) and postfixed in 1% OsO_4 in PBS. Then they were dehydrated in ascending ethanols and soaked in hexamethyldisilazane (Levanon and Stein, 1991, 1992, 1993), from which they were air dried. They were mounted on copper stubs with the joint apposing face laid upwards, coated with gold to give an 18 nm thick layer and visualized in a JEOL T-300 SEM (JEOL, Tokyo, Japan) operated at an accelerating voltage of 25 kV. Four synovial sectors were obtained from each rabbit: right (synovectomized) medial and lateral, and left (contralateral) medial and lateral. We studied each sector from each rabbit separately in the SEM and recorded all the morphological appearances, each in at least three standard magnifications so that records could present data on a comparable basis. Gross patterns were recorded in the ×35 magnification, and microarchitectural patterns were characterized in the ×3500 and ×20,000 magnifications.

A schematic drawing (Fig. 1) depicts the physical relationship between synovial linings and adjacent tissues of the joint.

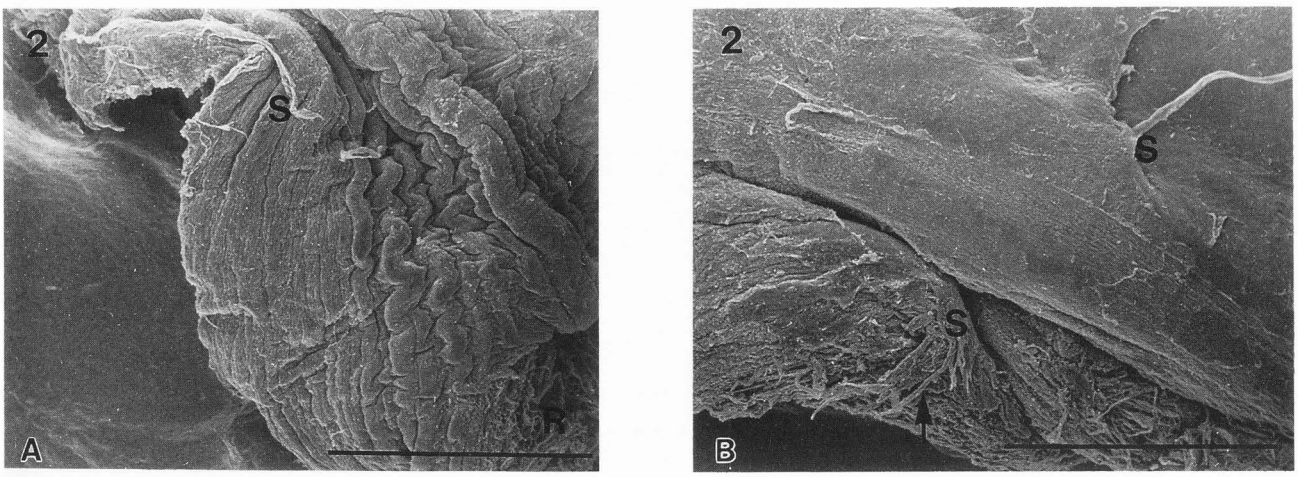

Figure 2. (**A**) Three weeks regeneration of left medial synovium: accordion-like pattern. Note curled ridges and a synoviophyte (S). Sieve bundles from an inner layer were exposed during resection (R). Bar = 1 mm. (**B**) Three weeks regeneration of right medial synovium: flat pattern. Note synoviophytes (S). The area denoted by an arrow harbors fibrillated areas, whose appearance was revealed under high magnification (cf. Fig. 9). Bar = 1 mm.

Table 2. Incidence and distribution of gross patterns of surface morphology on regenerating synovial linings.

Weeks Postop.	Morphologic Pattern Numbers* Control (Left) Knee Medial	Control (Left) Knee Lateral	Synovectomized (Right) Knee Medial	Synovectomized (Right) Knee Lateral
3	1, 2	1, 2	1, 2	1, 2
5	4	2	2	7
15	1	1	1	ND
15	1/7†	7	1, 2, 7	4
16	1, 7	ND	4, 5	1, 4, 7
16	1, 5	4, 5	2, 3	1, 2
17	2, 5	5	1, 2, 7	4
20	2, 5, 7	7	ND	1, 4
29	1, 4	1, 7	2, 6	6
29	1, 5, 7	2, 3, 5, 7	2, 6	1
36	2	2	1, 5	3
36	2, 3	1	5	2, 3
42	1, 5, 7	1, 5, 7	3	1, 7
44	5	5	2, 3	1, 2
44	4	4	1, 2	1, 2

ND = not determined

*Figures denote gross patterns of surface morphology as described in Table 1 and illustrated in Figures 2 to 7.

†Intermediate stage between patterns 1 and 7.

Results

Naked eye examination revealed synovial lining regeneration by 3 weeks after surgical ablation, at which time the tissue was still somewhat spongy and hyperemic. Synovial linings that were obtained 5 weeks and up to 44 weeks postoperatively appeared healthy and had a distinct vascular pattern.

Gross surface morphology of synovial linings

Examination under low-power SEM revealed a rich diversity of surface morphology. Seven main gross patterns are described in Table 1 and illustrated in parallel in Figures 2, 3, 4, 5, 6 and 7. These figures present gross patterns bearing some resemblance to, but still different from, those of intact synovia, which were previously described in detail (Levanon and Stein, 1992). Pattern 1, defined as an accordion-like pattern, is seen in Figure 2A. It was different from a similar pattern in the normal synovium, the latter having a generally uniform morphology consisting of regular, slender, straight, tightly packed ridges arranged in parallel along a given axis while the regenerating accordion was partly straight and partly with curled ridges (Fig. 2A). It was either loosely or tightly packed and in changing widths and divergent orientations (Figs. 3 and 4). Pattern 2, defined as a flat pattern, is seen in Figure 2B. The flat pattern was different from a similar pattern on normal synovia, on which it looked smooth and even, while on regenerating specimens the pattern was found to harbor outgrowths (Fig. 2B), to be corrugated (Fig. 3) and in places to be torn by deep cracks (Fig. 6). The fragile

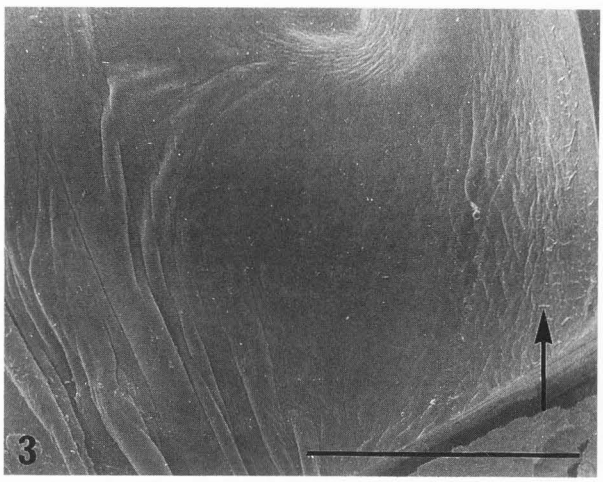

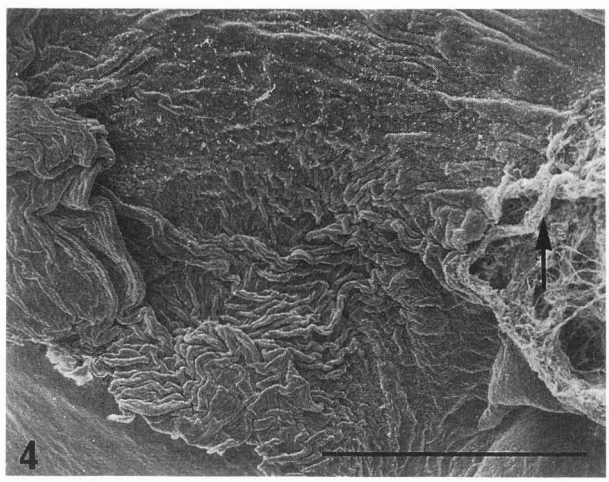

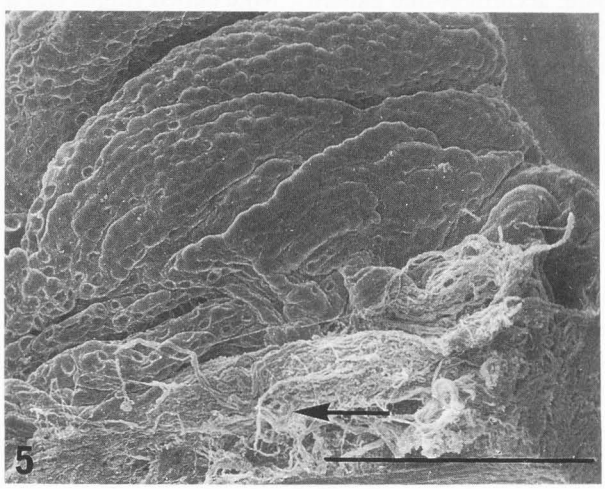

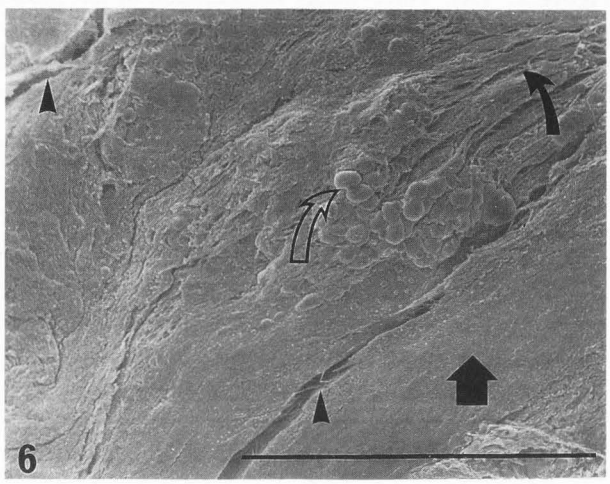

Figure 3. Sixteen weeks regeneration of right medial synovium: flat areas with random accordion-like ridges of changing orientation. Area on the right (arrow) was found under high magnification to exhibit thin, glistening coat covering sieve fibers, without masking the latter's contours (cf. Fig. 11). Bar = 1 mm.

Figure 4. Seventeen weeks regeneration of right lateral synovium: accordion-like ridges with variable orientations covering most of the surface. Note area with sieve bundles (arrow), which were exposed from underneath. These bundles were very poor in interfibrillar matrix. Bar = 1 mm.

Figure 5. Seventeen weeks regeneration of left lateral synovium: fatty areolar pattern. Note sieve bundles lacking interfibrillar material (arrow). Examination under high magnification revealed that this surface was almost totally covered by a bubble layer (cf. Figs. 12 and 13A). Bar = 1 mm.

Figure 6. Twenty-nine weeks regeneration of right lateral synovium: flat pattern with alternating smooth (solid, straight arrow) and rough areas. Note cracks of varying widths (arrowheads), fibrillated areas (solid, curved arrow), and gross adipocytes (open curved arrow). Bar = 1 mm.

---

appearances of the flat pattern on regenerating synovia bore clear-cut witness to stuttering rehabilitation. Pattern 5, defined as a fatty-areolar pattern, is seen in Figure 5. It resembled a similar pattern found on normal synovia. Pattern 6, defined as a flat pattern with alternating smooth and rough areas, is seen in Figure 6. This pattern differed from a similar pattern on normal synovia, the latter being characterized by a uniformly smooth surface, while the regenerated pattern bore alternating smooth and rough (fibrillated) areas and in places cracks. Pattern 7, defined as a lobe-like pattern, is seen in Figure 7. It was indistinguishable from a similar pattern found on normal synovia.

Figures 2A and 2B contained long and short projec-

Table 3. Microarchitectural patterns of synovial lining surface morphology.

Pattern/ Figure No.	Healing Time	Leg	Anatomical Sector	Description
A* (Fig. 9)	3 weeks	Syn	Lateral	Afibrillar ECM with irregular granules
B (Fig. 10)	16 weeks	Syn	Lateral	Straight or crimped collagen fibers, densely packed and studded with granules; only little afibrillar ECM was discerned
C (Fig. 11)	15 weeks	Con	Lateral	Fibers enmeshed in an open mat and coated by a thin, smooth, glistening layer; the latter obliterate the fibers' contours partially
D (Fig. 12)	44 weeks	Syn	Medial	Acellular processes branching out of shallow wand-like crests; the processes are skeins of fibers entangled in a torqued manner
E (Fig. 13)	36 weeks	Con	Medial	Bubble layer out of which evolve plates of "thorny" colonies
F (Fig. 14)	36 weeks	Syn	Lateral	"Thorny" plates covered by a thin, glistening coat
G (Fig. 16)	3 weeks	Syn	Medial	Cells bearing processes inlaid on a fibrillar mat
H (Fig. 17A)	16 weeks	Syn	Lateral	Flattened cells confluently coat the surface
I (Fig. 17B)	3 weeks	Syn	Medial	A mixed population of flattened and rounded cells confluently coat the surface
J (Fig. 18A)	20 weeks	Con	Medial	Synovial cells are partly covered by a bubble layer

Syn = Synovectomized (right) knee; Con = contralateral (control) knee; ECM = extracellular matrix.

*Capital letters denote microarchitectural patterns as described in the legends to Figures 9 to 14, and 16 to 18

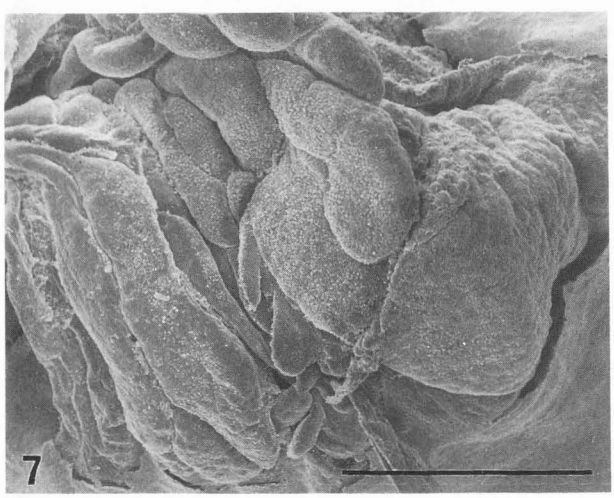

Figure 7. Twenty weeks regeneration of left lateral synovium: lobe-like pattern with lobes of different shapes and sizes. Examination under high magnification revealed that the character of this surface appeared to be intermediate between those of Figures 16B and 17B, i.e., an acellular coating from which cellular processes emerged onto the surface. Bar = 1 mm.

tions or outgrowths emerging from tissue folds and extending toward the surface. These outgrowths, for which we hereby propose the term "synoviophytes," were often recorded from regenerating synovial surfaces (Table 2) but were totally absent on intact specimens.

Very often, studying the surface of a given specimen showed that combination(s) of several gross patterns (Table 2) and/or their variations were present. This salient diversity in gross surface appearances was common in synovia obtained from experimental animals (both resected and contralateral joints, as detailed below) as opposed to those obtained from normal rabbits (Levanon and Stein, 1992).

Pattern 1 (accordion-like) and 2 (flat) appeared here as early as 3 weeks after synovectomy and were present on specimens sampled throughout the 44 weeks. Notably, the wealth of appearances marked all four sectors. However, the repertoire of patterns on each sector differed in incidence and course of development of patterns from that of the others.

Figure 8 depicts the development over time, in a cumulative manner, of the gross patterns 1-7 on each of the four synovial sectors {low magnification (×35) micrographs, Figs. 2 to 7, served to produce these stacked bar charts; the height of each of the bars was created by summing up the number of fields from a given specimen}. In Figure 8, it can be seen that the appearances (patterns) shown in Figures 2 and 7 were predominant all over the four sectors; pattern 6 was a minority on right-leg synovial linings and absent on left specimens, and the incidence of the other patterns was varied in the four sectors. The fatty-areolar pattern (Fig. 5) persisted on the left (contralateral) synovia, while it was completely absent on the right (regenerating) linings.

Table 4. Development with appearance of microarchitectural patterns of cellular and acellular fields.

Weeks Postop.	Microarchitectural Patterns* Left Knee Medial	Left Knee Lateral	Right Knee Medial	Right Knee Lateral
3	B, G, H, J	A/B†, B	B, G, I	A, A/B, B
5	A, B, I	A, G	A/B, B, J	A, I
15	A, B, I	C,‡ G§	A, J	B, C‡
15	J¶	J¶	B, D‡	A, A/B, B, G
16	A, G	ND	A, A/B, B, G, H	A, A/B, B, G, H
16	J¶	A/B, J	A, A/B, B, G	A/B, B, G
17	B, G, J	J¶	A, G, I	A/B, B
20	I, J	J¶	ND	A/B, J
29	J¶	G¶	B, J	A/B§,¶
29	G, J	G, I	G, I	A, A/B, G
36	E¶	B, F¶	F‡,¶	A, G
36	A¶	A¶	E, G‡‡	A, A/B
42	A/B, I	J¶	J¶	G, J
44	F,‡ G§	J§	E, J	I¶
44	E¶	G, H	A, A/B	J¶

ND = not determined

*Capital letters denote microarchitectural patterns as described in the legends to Figures 9, 10, 11, 12, 13, 14, 16, 17 and 18

†A/B = intermediate stage between A and B

‡This pattern was not included in Figure 15, being a rare (albeit significant) appearance

§Giant adipocytes of 90 μm in one dimension were present

¶All the surface was uniformly covered by this pattern

‡‡Other sections of this area were covered by bubble layer. This was a rare case in which bubble material did not uniformly cover a specimen, thus enabling discernment of cellular surfaces

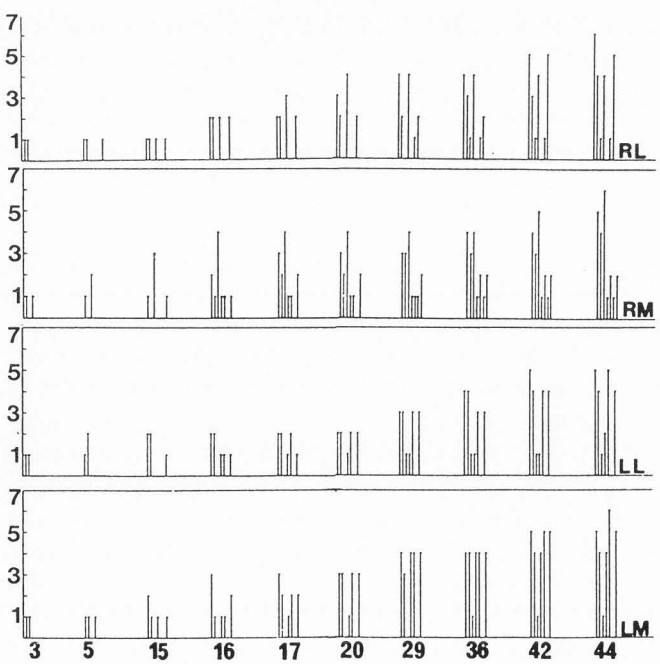

Figure 8 (at left). Stacked bar chart showing cumulative development of gross patterns on regenerating and contralateral synovial surfaces after ablation. Numbers on the abscissa denote recuperation intervals in weeks (not depicted to scale). Numbers on the ordinate denote the summed score of appearance of gross patterns throughout an actual recuperation time interval. The height of each of the bars represents the number of fields recorded in the ×35 magnification. Each time interval may contain from two to seven (e.g., RM, 44 weeks) bars, each of which represents, when read from left to right, the following patterns: 1: accordion, 2: flat, 3: flat with random accordion ridges, 4: accordion made out of ridges with alternating orientations, 5: fatty areolar, 6: flat with alternating smooth and rough areas and 7: lobe-like. The numbers are identical to those of the figures depicting these patterns. LM: left medial; LL: left lateral; RM: right medial; RL: right lateral.

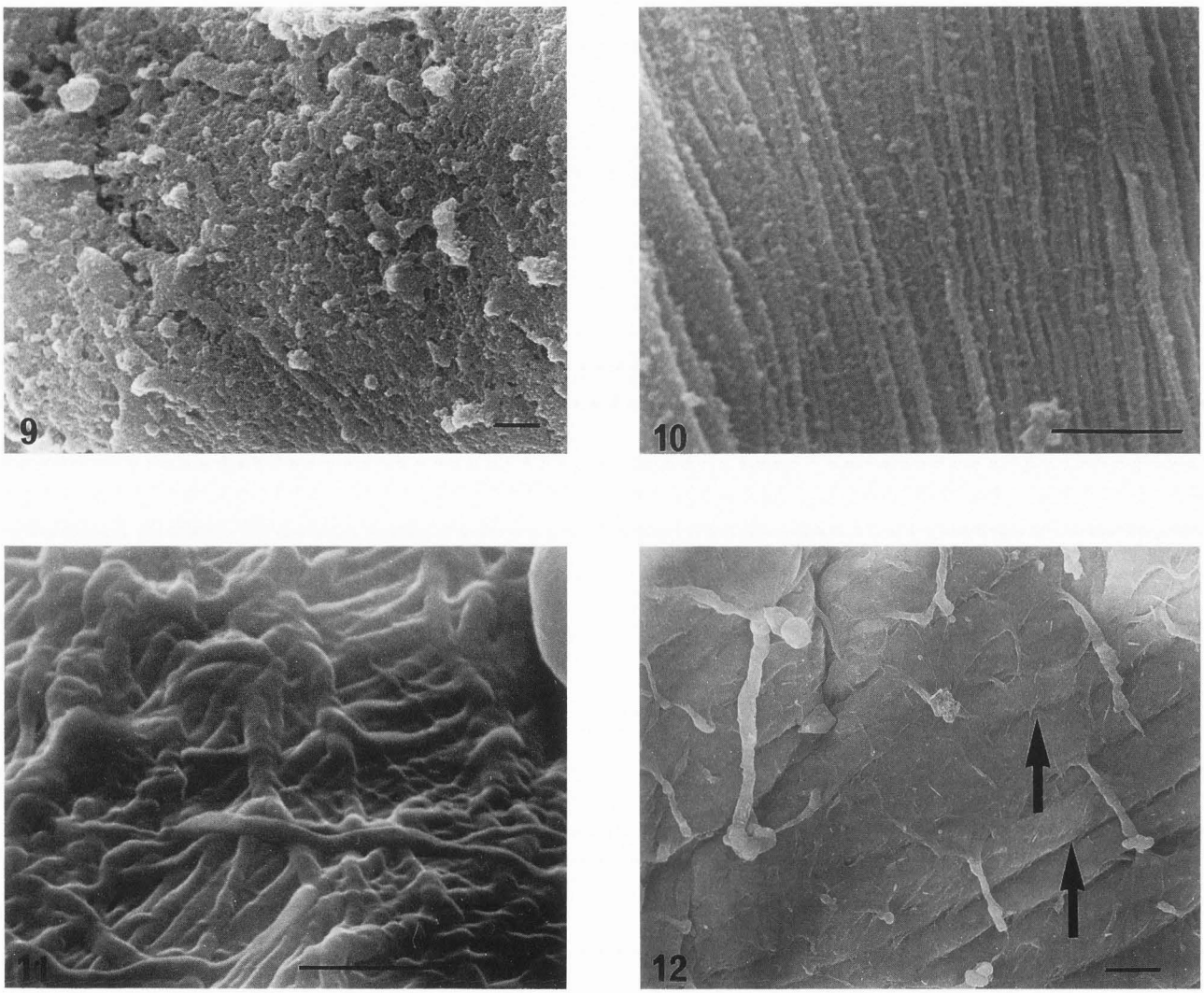

Figure 9. Three weeks regeneration of right lateral synovium: acellular pattern A, with afibrillar material composed of amorphous groundwork with irregular granules of changing dimensions. No fibrillar structures were depicted on this pattern. Examination under low magnification revealed crests arranged in parallel, after the accordion pattern (cf. Fig. 2A). Bar = 1 μm.

Figure 10. Sixteen weeks regeneration of right lateral synovium: acellular pattern B, with straight or curled sieve fibers, densely packed in bundles or arranged like "matches in a box" and studded with granules. This pattern was predominant on surfaces that appeared poor in afibrillar material (Figs. 2A, 4, 5 and 6) but was very sparse on surfaces of intact synovial linings. Bar = 1 μm.

Figure 11. Fifteen weeks regeneration of left lateral synovium: acellular pattern C, with fibers entangled in an open hammock and coated by a thin glistening layer. The latter does not mask fibrillar contours, yet it reduces their sharpness. Bar = 1 μm.

Figure 12. Forty-four weeks regeneration of right medial synovium: acellular pattern D, with long and short acellular processes of various shapes and sizes aligned in a generally uniform orientation and branching out of wand-like structures (arrows) oriented at 90° to the processes (seen also in low power in Fig. 3, right side). Careful examination under high power revealed that the processes were not effete cells but skeins of fibers entangled in a torqued manner and enmeshed in amorphous extracellular matrix. Bar = 10 μm.

Microarchitecture at high magnification

Table 3 presents a description of the micropatterns. Table 4 summarizes the incidence of the microarchitectural patterns in each of the four sectors during regeneration. Two general patterns were visualized: acellular and cellular. Major and/or minute variations in these patterns were recorded in close proximity to one another on the same field, on adjacent fields or on other fields elsewhere.

Acellular patterns Examination of synovial surfaces at magnifications ranging from ×2,500 to ×20,000 showed a wide diversity of acellular patterns; the principal ones are presented in Figures 9, 10, 11, 12, 13 and 14. Figure 15 shows the development over time, in a cumulative manner, of these patterns {as with Fig. 8, the height of each of the stacked bars in Fig. 15 was produced by summing up the medium (×350), or the high (×3500), magnification micrographs recorded from a given specimen}. These consisted of either (**1**) afibrillar matrix (cf. Fig. 9), (**2**) fibrillar bundles with sharp contours studded with granules of various dimensions and changing incidence (Fig. 10) or (**3**) fibrillar bundles with a thin coating that did not hamper visualization of typical fibrillar contours (Fig. 11). Acellular pattern D (Fig. 12) was interesting: this pattern was not seen on intact specimens but, surprisingly, resembled appearances recorded from articular surfaces of load-bearing sectors from normal rabbits (cf. Figs. 2B, 4 and 6 in Levanon and Stein, 1991).

Also present was a bubble layer (Fig. 13, pattern E) similar to that described previously (Levanon and Stein, 1992), but in the present study it was accompanied in places by related structures (Fig. 13) which were not recorded before. Significantly, the bubble layer appeared only at a late stage and was confined to four medial specimens (36 and 44 weeks). In contrast, on intact linings it consisted of as much as 70% of the total synovial area. Since acellular pattern F (Fig. 14) was found only on bubble layer, it seems possible that the thorns' coating was derived from or related to the bubble material as well. However, uncoated and bubble-coated thorny colonies were never found on the same specimen, which might suggest some distinct differences in surface biochemistry and/or organization and could justify, at least at present, a separate pattern.

Vast fibrillated areas (i.e., areas which harbored fibrillar bundles with only little, if any, interfibrillar material, e.g., Fig. 10) were recorded. These were found both at the margins (Figs. 2, 4 and 5) and in the center (Fig. 6) of the examined specimens and were not restricted to any given gross pattern, to any sector of either joint or to any stage of recuperation. Therefore, we tend to consider it as a pattern existing *in situ*, rather than as an artifact brought about during preparation for the SEM. In contrast, on specimens from intact rabbits (Levanon and Stein, 1992) this appearance was limited to small, rare fields. Notably, the accordion-like (Fig. 2A) and the flat (Fig. 2B) patterns contained mostly fibrillated fields.

Cellular patterns Two main types of cells, depicted in Figures 16, 17 and 18 were found to coat synovial surfaces either confluently or discontinuously. One type consisted of rounded cells protruding from the surface toward the joint cavity (Figs. 16B and 17B), and the second type consisted of well-spread dendrite-like synoviocytes (Fig. 17A). In places, bubble layer was found to thinly coat synovial cell surfaces (Fig. 18B).

Relationship between regenerating and contralateral synovia

Regenerating and contralateral specimens resembled each other in presenting an abundance of surface patterns (Figs. 8 and 15, Tables 2 and 3), a finding which is significant and novel. Gross and microarchitectural patterns of regenerating and contralateral synovia were found to bear cardinal differences from those of intact rabbits, with the pattern categories of the former outnumbering those of the latter. For example, out of 20 intact synovial specimens studied (Levanon and Stein, 1992), 10 showed a single gross pattern, while the other 10 contained only two additional patterns. This differed from regenerating and contralateral synoviae, in which the diversity was much wider, as shown in Table 4.

No correlation between gross patterns and microarchitectural patterns, on any of the synovial specimens, at any time interval, could be shown.

Relationship between synovia from ablated and sham-operated joints

Two rabbits which were sham-operated and whose synoviae were sampled after 8 weeks recovery time, served as controls. Medial and lateral synoviae of both right and left joints all showed the flat and lobe-like gross patterns. In addition, in synovia from sham-operated rabbits, the flat pattern appeared in places with moderate corrugations, and in two instances aggregates of very large (50-120 μm in one dimension) adipocytes were recorded. At high magnification, all the specimens of sham-operated synoviae were found to be coated by the bubble layer.

Discussion

Synovial regeneration

Early studies on the regeneration of synovial linings in healthy animals indicated that normal-appearing synovia with distinctive ultrastructure regenerated within 40-100 days postoperatively (Mitchell and Blackwell, 1968;

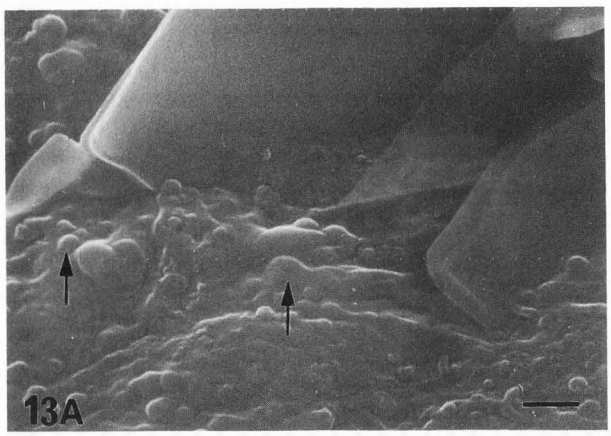

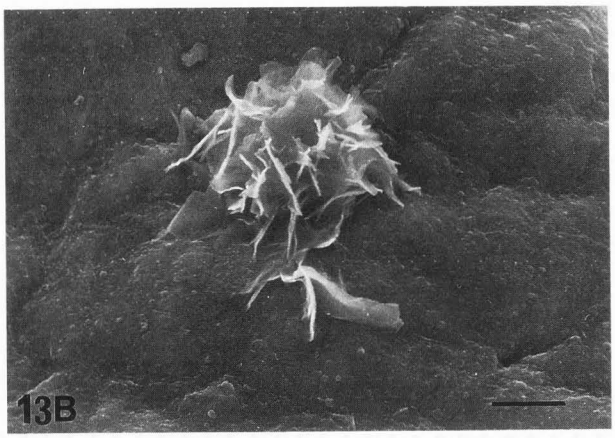

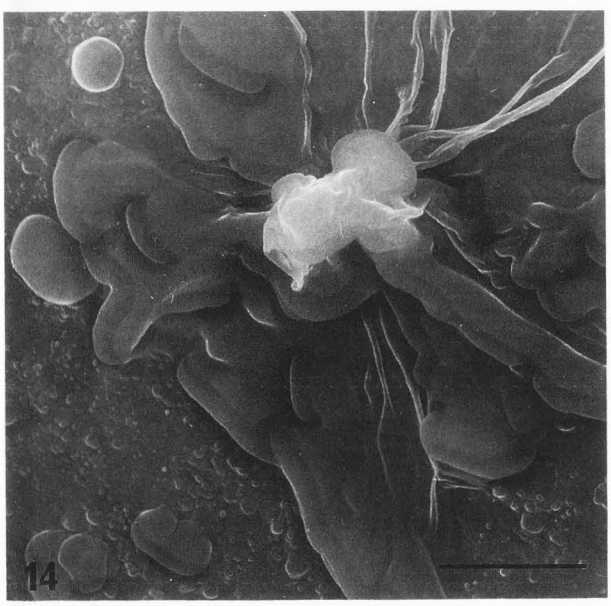

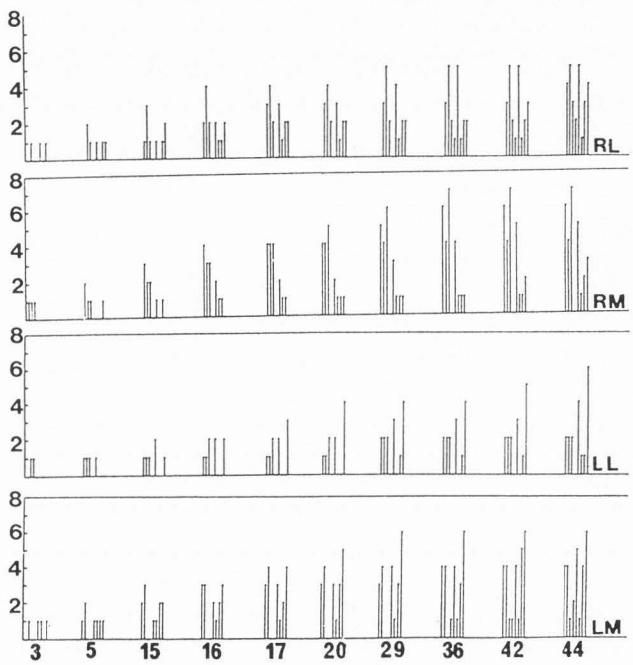

Figure 13. Thirty-six weeks regeneration of left medial synovium: acellular pattern E with bubble layer. **(A)** Note confluent layer of bubbles or "pebbles" of various shapes and dimensions (arrows), out of which lamellae or plates of "thorny" colonies evolve. Thorny lamellae looked glistening and very smooth, even when examined under magnification as high as ×100,000 (not shown). Bar = 1 μm. **(B)** Same area as in (A) at lower magnification. Note a colony of lamellae intermingled with one another, evolving from a bubble layer which at this magnification looks almost entirely smooth. Fields of bubble layer were found with or without lamellar thorns. Bar = 10 μm.

Figure 14. Thirty-six weeks regeneration of right lateral synovium: acellular pattern F, with acellular structures resembling thorny plates, covered by a thin, smooth and glistening coating that does not hamper visualization of thorny contours (cf. pattern C, Fig. 10) and found only on bubble layer surfaces. Bar = 10 μm.

Figure 15. Stacked bar chart showing microarchitectural patterns on regenerating and contralateral synovial surfaces after ablation. Numbers on the abscissa denote recuperation intervals in weeks (not depicted to scale). Numbers on the ordinate denote the summed scores of appearances of microarchitectural patterns throughout an actual recuperation time interval. The height of each of the bars represents the number of fields recorded in the ×35 magnification. Each time interval may contain from two (e.g., LL, 3 weeks) to seven (e.g., LM, 44 weeks) bars, each of which represents, when read from left to right, the following micropatterns: 1: pattern A (see **Microarchitecture at high magnification** in **Results**), 2: pattern B, 3: pattern A in conjunction with B, 4: pattern E, 5: pattern G, 6: pattern H (see Fig. 17A), 7: pattern I (see Fig. 17B) and 8: pattern J (see Fig. 18). LM: left medial; LL: left lateral; RM: right medial; RL: right lateral.

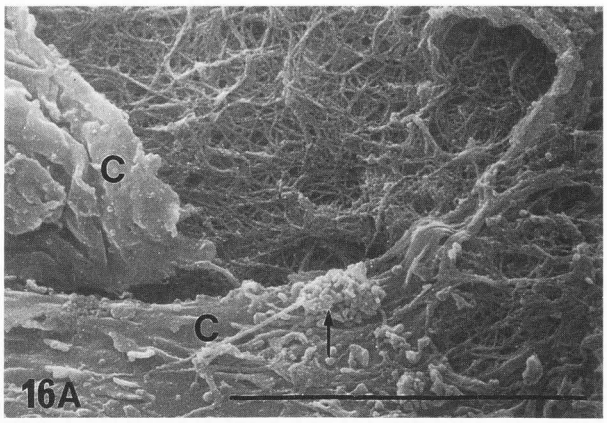

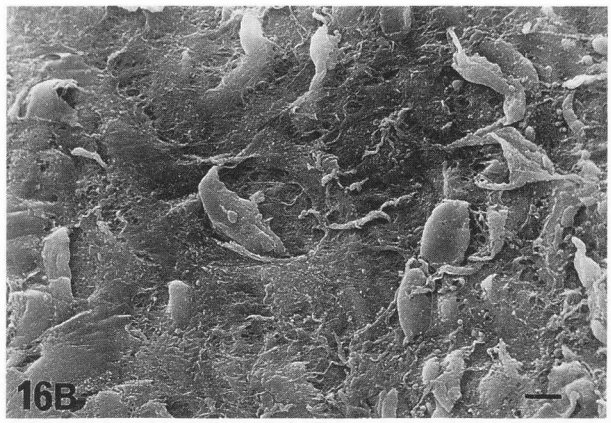

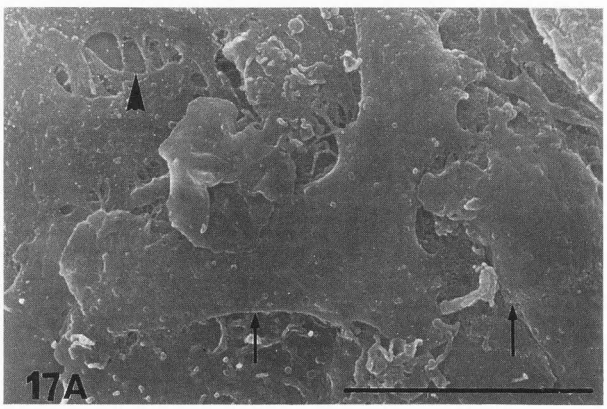

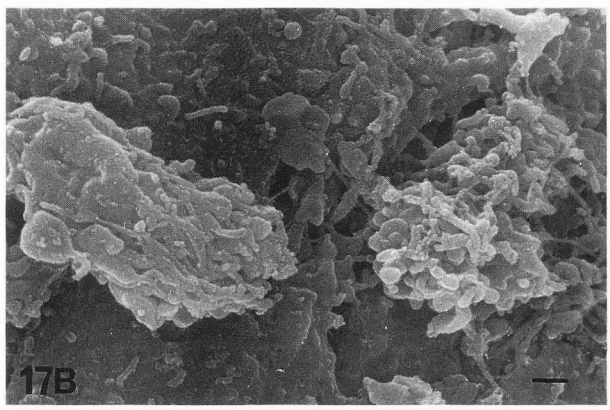

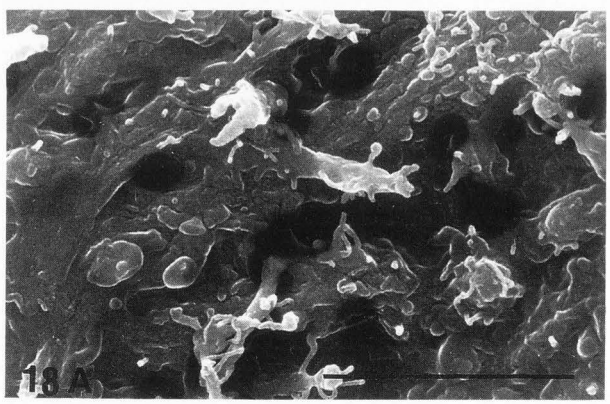

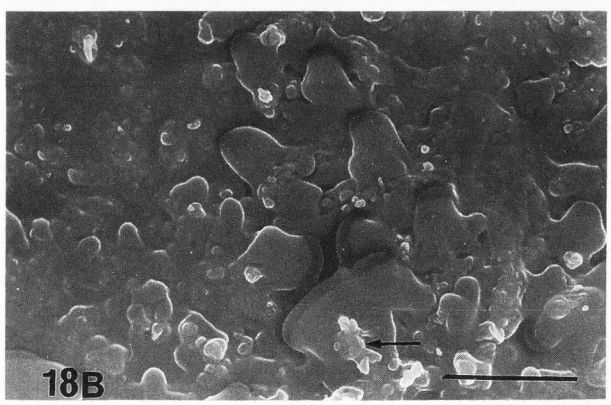

Geens, 1969; Bentley *et al.*, 1975; Kim and Moon, 1979). In the present study, a considerable synovial mass, if an imperfect one, was present as early as 21 days following synovectomy.

Surface morphology of regenerating synovia in the operated rabbit

Three findings presented here are of central significance. The first concerns the characteristic surface morphology of the regenerated synovial linings throughout the rehabilitation period. The second is the absence of normal-appearing surface morphology on the regenerated synovia by 44 weeks (Tables 4 and 5). The third point relates to the surface morphology of the contralateral synovia, which resembled that of the regenerated rather than that of control, normal linings.

The features of regenerated synovia, as opposed to those of control specimens, consisted of an abundant repertoire of gross and microarchitectural patterns. Surface morphology patterns, predominant on regenerating synoviae but absent on intact and sham-operated specimens, included poorly organized accordion areas, vast fibrillated arenas, synoviophytes, rare and delayed appearance of bubble layer, corrugated and cracked areas of the flat pattern. This seems to indicate either retarded morphological regeneration or, possibly, functional regeneration as well.

Figure 16. Three weeks regeneration of right medial synovium: cellular pattern G. **(A)** Note cells (C) bearing processes (arrow) and which are inlaid on a fibrillar mat. The latter looks like an open basket. Under high magnification, the sieve fibers were found to harbor numerous granules, as in Figure 9. Bar = 10 μm. **(B)** Same area as in (A) at lower power. Note cells that coat the surface inconfluently. Some of the cells tend to be rounded and detached from the surface. Bar = 10 μm.

Figure 17. **(A)** Sixteen weeks regeneration of right lateral synovium: cellular pattern H, showing flattened cells with few and short processes confluently coating the surface. In some places, cell borders are discernible (arrows) and in others, adjacent cells are united by finger-like interdigitations (arrowhead). Bar = 10 μm. **(B)** Three weeks regeneration of right medial synovium: cellular pattern I, with confluent synovial cells coating vast areas which do not seem to bear extracellular matrix anywhere. Cells are either flattened or rounded, generally with well-developed cell processes. In some places, rounded cells are partly detached from the surface. Bar = 10 μm.

Figure 18. **(A)** Twenty weeks regeneration of left medial synovium: cellular pattern J, with synovial dendritic cells that are partly covered by a bubble layer coating vast areas. Bar = 10 μm. **(B)** Forty-four weeks regeneration of right medial synovium. Synovial cells are almost completely covered by bubble material, leaving only scarce cell processes evolving onto the surface (arrow). Bar = 10 μm.

Table 5. Comparison of numbers of gross and microarchitectural patterns on intact and regenerating synovial specimens.

	Intact*			Regenerating†		
Pattern No.	Number of Specimens	Gross‡ (%)	Micro§ (%)	Number of Specimens	Gross¶ (%)	Micro**
1	10	50		21	37	
2	10	50		27	47	
3				7	12	
4				2	4	
1	13		65			30
2	1		5	26		45
3	5		25	10		17
4	1		5	3		5
5				2		3

*Data for normal synovial specimens were taken from our study of intact rabbits (Levanon and Stein, 1992).
§Percentage of microarchitectural patterns on intact synovia. †Data taken from present study.
¶Percentage of gross patterns on regenerating synovia. ‡Percentage of gross patterns on intact synovia.
**Percentage of microarchitectural patterns on regenerating synovia.

A second interesting observation is that normal-appearing surface morphology was not present by 44 weeks postoperatively, at which time biomechanical equilibrium might well have been reestablished. The failure of regenerated synovia to resume normal-appearing surface morphology probably lies in the absence of synoviocytes able to restart the highly controlled biosynthesis and assembly of the specific compounds of synovial extracellular matrix (Kühn, 1986). Laxity induced in the hind joints has been reported to have ultimately generated fibrillated areas on cartilages (Ghosh *et al.*, 1990). Fibrillation is a structure of native, thin collagen fibers which lose accompanying proteoglycan macromolecules, subsequently collapse and fuse to form thicker fibers, which are evident on SEM. This impairment cannot be reversed or rectified since reconstruction of a biomechanically functional matrix requires removal of collapsed collagen and the presence of synoviocytes able to restart the highly controlled biosynthesis of normal matrix constituents. Failure to meet these requirements in injured synovial linings means that regenerated synovia in the adult rabbit cannot be expected to imitate the native synovia. Hence, an abnormal surface morphology is recorded in regenerating synovia.

In evaluating the morphology of the contralateral synovia, different considerations arise. Independent studies in experimental models of joint laxity (not based on a direct insult to synovial linings) collectively indicated that lesions and altered biosynthesis of proteogly-

cans in synovial joint cartilages were a direct consequence of impaired mechanical equilibrium in the joint (McDevitt *et al.*, 1977; Caterson and Lowther, 1978; Myllala *et al.*, 1983; Vignon *et al.*, 1987; Ghosh *et al.* 1990; Robinson *et al.*, 1992). Both synovia and articular cartilage share a prime function in absorbing and moderating the mechanical load and compression cycles in the synovial joint during motion. This role can be fulfilled provided that the unique combination of native collagen fibers and proteoglycan macromolecules, delicately interwoven with one another, is maintained. Under intense mechanical stress, disruption of macromolecular organization of extracellular matrix takes place, resulting in fibrillation (Kühn, 1986).

Surface morphology of the synovia from the sham-operated rabbits was indistinguishable from that of intact rabbits (cf. Levanon and Stein, 1992); the dominant lobe-like and bubble layer patterns persisted here, too; no appearance of fibrillation or synoviophytes was discerned. This clearly indicates that only removal of synovial tissue (not merely a cut in the skin, no matter how deep) can elicit the morphological changes described here.

Previous reports on chemical analyses of articular cartilages in immobilized versus contralateral joints of rabbits (Taami *et al.*, 1983; Burr *et al.*, 1984) and sheep (Caterson and Lowther, 1978) revealed degradative changes in glycosaminoglycans and collagen in both joints. These biochemical changes were accounted for by the joint response to a change in functional demand. Typically, the proteoglycans isolated from the non-load-bearing articular cartilages were of lower molecular weight; deterioration lessened the entanglement between proteoglycans and collagen fibrils after the manner of the stag caught in the thicket (Ghadially, 1983) and underlay their leakage and loss from the tissue (Pottenger *et al.*, 1982; Hunziker, 1991). Increased extractability of proteoglycans from cartilage has been reported to result primarily from loss of integrity of the collagen mesh, rather than from disruption of proteoglycan aggregates (Pottenger *et al.*, 1982).

In conclusion, synovectomy in the rabbit knee was shown to result in regeneration of a marked synovial mass 3 weeks following resection. The surface morphology of this newly developed tissue differed greatly from that of normal synovial lining, and the latter had not been restored by as late as 44 weeks postsynovectomy. Moreover, the contralateral synovia closely resembled in surface morphology the regenerated specimens rather than the normal ones. This resemblance can be explained on the basis of the alteration of mechanical equilibrium in the contralateral joint. Very likely, additional yet unaccounted for factors operate in the newly formed synovial lining (Lohmander, 1991). This last finding precludes referring to the contralateral knee as an intact control.

Acknowledgments

We thank Miss Ruth Singer for editing and excellent typing of this article. We are grateful to Dr. Varda Gottfried for her help in preparation of Figures 8 and 15 and to Professor I. Nir for critical reading and many helpful suggestions during preparation of the manuscript.

References

Bentley G, Kreutner A, Ferguson AB (1975) Synovial regeneration and articular cartilage changes after synovectomy in normal and steroid-treated rabbits. J Bone Joint Surg **57B**: 454-462.

Burr DB, Frederickson RG, Pavlinch C, Sickles M, Burkhart S (1984) Intracast muscle stimulation prevents bone and cartilage deterioration in cast-immobilized rabbits. Clin Orthop Relat Res **189**: 264-278.

Caterson B, Lowther DA (1978) Changes in the metabolism of the proteoglycans from sheep articular cartilage in response to mechanical stress. Biochim Biophys Acta **540**: 412-422.

Frizziero L, Georgountzos A, Zizzi F, Focherini MC (1992) Microarthroscopic study of the morphologic features of normal and pathological synovial membrane. Arthroscopy **8**: 504-509.

Gamliel H, Gurfel D, Leizerowitz R, Poliak A (1983) Air drying of human leukocytes for scanning electron microscopy using the GTGO procedure. J Microsc **131**: 87-95.

Gardner DL (1991) Pathological Basis of Connective Tissue Diseases. Edward Arnold, London. p. 966.

Geens S (1969) Synovectomy and debridement of the knee in rheumatoid arthritis. J Bone Joint Surg **51A**: 617-625.

Ghadially FN (1983) Fine Structure of Synovial Joints. Butterworths, London. pp. 4, 45, 75.

Ghosh P, Sutherland J, Bellenger C, Read R, Darvodelsky A (1990) The influence of weight-bearing exercise on articular cartilage of menisectomized joints. Clin Orthop Relat Res **252**: 101-113.

Hunziker EB (1991) Tissue sampling and preservation for morphological studies. In: Methods in Cartilage Research. Maroudas A, Kuettner K (eds.). Academic Press, London. pp. 19-25.

Kim JN, Moon MS (1979) Effect of synovectomy upon regeneration of meniscus in rabbits. Clin Orthop **141**: 287-294.

Kühn K (1986) Part I: Cartilage matrix components. Introduction. In: Articular Cartilage Biochemistry. Kuettner KE, Schleyerbach R, Hascall VC (eds.). Raven

Press, New York. pp. 1-2.

Laurin CA, Desmarchais J, Daziano L, Gariepy R, Derome A (1974) Long-term results of synovectomy of the knee in rheumatoid patients. J Bone Joint Surg **56A**: 521-531.

Levanon D, Stein H (1991) The articular cartilage of the rabbit knee: A scanning electron microscopy study. Cells Mater **1**: 219-229.

Levanon D, Stein H (1992) The synovial lining of the rabbit knee: A scanning electron microscopy study with specimens reinforced with tannic acid. Histochem J **24**: 25-32.

Levanon D, Stein H (1993) Evaluation of the use of tannic acid in preparation of the rabbit knee meniscus for scanning electron microscopy. Scanning Microsc **7**: 741-750.

Lohmander LS (1991) Osteoarthritis: Man, models and molecular markers. In: Methods in Cartilage Research. Maroudas A, Kuettner K (eds.). Academic Press, London. pp. 337-362.

McDevitt C, Gilbertson E, Muir H (1977) An experimental model of osteoarthritis: Early morphological and biochemical changes. J Bone Joint Surg **59B**: 24-35.

McEwen C (1988) Multicenter evaluation of synovectomy in the treatment of rheumatoid arthritis: Report of results at the end of five years. J Rheumatol **15**: 764-769.

Mitchell N, Blackwell P (1968) The electron microscopy of regenerating synovium after subtotal synovectomy in rabbits. J Bone Joint Surg **50A**: 675-686.

Myllala T, Peltonen L, Puranen J, Kalevi Korhonen L (1983) Consequences of synovectomy of the knee joint: Clinical, histopathological and enzymatic changes and changes in 2 components of complement. Ann Rheum Dis **42**: 28-35.

Pottenger LA, Lyon NB, Hecht JD, Neustadt PM, Robinson RA (1982) Influence of cartilage particle size and proteoglycan aggregation on immobilization of proteoglycans. J Biol Chem **257**: 11479-11485.

Robinson D, Halperin N, Nevo Z (1992) Devascularization of the anterior cruciate ligament by synovial stripping in rabbits. Acta Orthop Scand **63**: 502-506.

Stein H (1976) The Inter-relationship of Synovium and Articular Cartilage. D. Phil. Thesis. University of Oxford, England.

Taami M, Säämänen AM, Jauhiainen A, Malminen O, Kirivanta E, Helminen H (1983) Proteoglycan alterations in rabbit knee articular cartilage following physical exercise and immobilization. Connect Tissue Res **11**: 45-55.

Vignon E, Bejui J, Mathieu P, Hartman D, Ville G, Evreux JC, Descotes J (1987) Histological cartilage changes in a rabbit model of osteoarthritis. J Rheumatol **14**: 104-106.

Discussion with Reviewers

D.L. Gardner: Is it possible to give an indication of the proportion of each joint in which each of the seven categories was shown? It is appreciated that whole synoviums were not sampled for SEM, but it might prove possible to tabulate a result such as, e.g., 30% of surfaces examined at 3 weeks showed pattern 2, whereas 55% of surfaces showed pattern 4 at 17 weeks. Either absolute or relative measurements would be of interest.
Authors: This kind of morphometric analysis was not done in this study since several specimens had somewhat tortuous geometry, and thus not all the joint apposing surfaces were revealed to the scanning beam at 0° inclination to the stub holder. The proportion of tilted and/or hidden surfaces could not be assessed with certainty, therefore the relation between the actual surface of a given specimen and its projection on the stub was unknown. Presentation of quantitative data as suggested by the reviewer may find insufficient foundation in our crude data. Still, within presently feasible methods, Tables 1 and 2 depict the gleaned data exhaustively.

D.L. Gardner: Were any conventional light microscopic preparations made that could help clarify the ultrastructural records? In Figure 2A, the regenerated material is clearly dominated by arrays of crimped collagen bundles, and in Figure 7 the villous synovial structure is apparent. However, in other places (Figs. 3, 6, 10 and 17A), it would be of value to see this material cut in perpendicular sections and stained conventionally.
Authors: Production of histochemical preparations was considered, but was not adopted for several reasons. Collagen fibers, straight and/or crimped, had already been shown on semithin sections of synovial linings, as had glycosaminoglycans (GAG) (Scott, 1985; Levanon and Stein, 1992, and refs. cited therein). Specific GAG or proteoglycan stainings, e.g., critical dye concentration, would probably yield crude histochemical data whose study might require a separate publication. The situation of the bubble layer pattern (Fig. 13) is different; this pattern was discovered and dealt with broadly by us (Levanon and Stein, 1992), presenting evidence that indicated high lipid content. However, its biochemical nature was not clarified, and a standard histochemical staining for light microscopy has not been worked out. The possible contribution of histochemical sections seems too little or beyond the scope of this SEM study.

Figures 3 and 6 depict fields coated by afibrillar extracellular matrix in low magnification; Figure 10 depicts sieve fibers which harbor sparse but discernible interfibrillar structures {the relationship between the latter and similar structures, dealt with in detail by us (Levanon and Stein, 1995), requires a separate study} in high

magnification. Figure 17A presents flattened synoviocytes, perpendicular sectioning of which would likely reveal their intracellular structure, a subject first described over 30 years ago by Cochrane *et al.* (1965); many publications have appeared since (e.g., Wyllie *et al.*, 1964; Highton *et al.*, 1968; Burmester *et al.*, 1983; Hendler *et al.*, 1985; McDonald and Levick, 1988; Levick and McDonald, 1990). However, surface morphology not intracellular structures, is the focus of the present study.

D.L. Gardner: The authors have correctly surmised that the normal and abnormal ultrastructure of the rabbit, human and other joints, are closely similar, but how do they relate in chronological terms? If the rabbit synovium is well reformed by 44 weeks, can this time scale be extrapolated to both mouse and human?
Authors: We mention the close ultrastructural similarity between human and rabbit synovial linings, after Ghadially (1983). Mouse and other mammals were not dealt with. This reference was used to explain why the rabbit synovia were chosen as an experimental model that enables not only comparison with humans but also convenient sampling of the whole synovial tissue. However, the results of the present study indicate that regenerated synovial mass is not a structural, and potentially not functional, copy of original synovial lining, no matter how long the animal rebuilt it. Also, the surface morphology of the unresected contralateral synovial linings suffered wholesale degradative changes. These outcomes might apply to humans and other mammals, yet species specific differences in structural synovial components, posture and gait have to be taken into account, i.e., surface morphology of mammalian genera can be likened, but identity has to be found experimentally.

K.D. Draenert: The specimens presented seem to be air dried. This is a rather rough procedure.
Authors: The specimens were air dried from hexamethyldisilazane as described by Nation (1983) and cited by us (Levanon and Stein, 1991, 1992, 1993). This procedure has been shown to be most effective in preserving fragile surface details. It is based on the use of an intermediate solvent whose critical point is very close to room temperature and atmospheric pressure, thus avoiding the high pressure, which is inevitably exercised in critical-point drying from, e.g., carbon dioxide. Our method is therefore harmless to susceptible specimens.

Additional References

Burmester GR, Locher P, Koch B, Winchester RJ, Dimitriu-Bona A, Kalden JR, Mohr W (1983) The tissue architecture of synovial membranes in inflammatory and non-inflammatory joint diseases: The localization of major synovial cell populations as detected by monoclonal reagents directed towards Ia and monocyte-macrophage antigens. Rheumatol Int **3**: 173-181.

Cochrane W, Davies DV, Palfrey AJ (1965) Absorptive functions of the synovial membrane. Ann Rheum Dis **24**: 2-15.

Hendler PL, Lavoie PE, Werb Z, Chan J, Seaman WE (1985) Human synovial dendritic cells: Direct observation of transition to fibroblast. J Rheumatol **12**: 660-664.

Highton TC, Myers DB, Rayns DG (1968) The intercellular spaces of synovial tissue. N Z Med J **67**: 315-325.

Levick JR, McDonald JN (1990) Microfibrillar meshwork of the synovial lining and associated broad-banded collagen: A clue to identity. Ann Rheum Dis **49**: 31-35.

McDonald JN, Levick JR (1988) Morphology of surface synoviocytes *in situ* at normal and raised joint pressure, study by scanning electron microscopy. Ann Rheum Dis **47**: 232-240.

Nation (1983) A new method using hexamethyldislazane for preparation of soft insect tissues for scanning electron microscopy. Stain Technol **58**: 347-351.

Scott JE (1985) Proteoglycan histochemistry: A valuable tool for connective tissue biochemists. Collagen Res **5**: 541-575.

Wyllie JC, More RH, Haust MD (1964) The fine structure of normal guinea pig synovium. Lab Invest **13**: 1254-1263.